# An Adaptive HV Transmission Lines Reclosing based on Voltage Pattern in the Complex Plane

M.R. D. Zadeh, I. Voloh, Mital Kanabar, GE Digital Energy
Y. Xue, American Electric Power

***Abstract*—Transient single-phase short circuits are the most common transmission line faults. The short circuit arc of a transient fault is usually self-extinguishing after opening the line circuit breakers. High-speed single-phase reclosing of transmission line can help to improve system stability. Employing a pre-set reclosing interval may pose problem if the time interval is not sufficient to fully deionize the fault arc. It is desirable to have adaptive reclosing interval and fast detection of arc extinction, which could facilitate successful high-speed reclosing of transmission line and bring benefit to the system stability. A new adaptive reclosing algorithm is proposed in this paper. It uses the pattern of the faulted phase voltage in the complex plane to distinguish between transient and permanent faults and is also able to detect the time when the arc is extinguished. Theoretical analysis is provided to support the technique. In addition, the performance of the proposed technique is verified using a recorded field data from 765 kV transmission line and several cases simulated in EMTP including detailed arc and CVT modeling.**

***Index Terms*— Adaptive Single-Phase Reclosing, Secondary Arc Extinction, Four-legged Shunt Reactor Compensation, EMTP Simulation.**

## I. Introduction

For Extra and Ultra High Voltage (EHV, UHV) transmission lines, the setting of reclosing time interval is based on the maximum deionization duration of fault arc [1] and other system requirements. . For high voltage transmission systems, short circuit capacity of the system usually increases with the higher system voltage level. The higher short circuit power results in higher fault current and longer arc extinction time that requires the reclosing time interval to be extended to allow deionization of the air gap at the fault point [2]. Application of single-phase reclosing helps to increase the system stability limit as system voltage and short circuit level increase.

According to statistics, more than eighty percent of transmission line faults are single-phase to ground faults and a high percentage of these faults are of transient type. Therefore, most of the line faults could be cleared by using high speed automatic single-phase reclosing. If arc is extinguished completely before the first shot of reclosing, the chance of successful reclosing would be maximized.

In order to have successful high speed reclosing, different methods have been applied to extinguish the arc faster. One of the common methods is to use a four-legged shunt reactor at each end of the line. By appropriate selection of neutral reactor, the arc current can be limited and extinguished fast [3], [4]. This method is more effective for transposed lines than untransposed lines. Whereas, use of a four-legged reactor at one end and another four-legged reactor with switching scheme has been applied for untransposed lines at very high voltage levels [4][5].

Fixed reclosing interval setting is applied to majority of transmission lines. It may cause problem if the time interval is not sufficient to fully deionize the fault arc. The reclosing before arc extinction results in arc restrike and could cause the line protection to trip again, which may incur more stress to the power system. Under certain conditions, the reclose-onto-fault may put system stability at risk or damage the equipment. Hence it is desirable to have adaptive high-speed reclosing that uses variable open time interval to allow the breaker to close only after the fault arc has extinguished.

Most of the techniques available or presented in the literature for adaptive reclosing are based on harmonic components of faulted phase voltage taken after breaker tripping [6][7][8]. These techniques were tested on transmission lines under certain system configurations. However, the pattern of the faulted phase voltage and its harmonic components varies drastically when transmission line is transposed, partially transposed or untransposed, shunt compensated with four-legged reactor that may or may not have switching capability. Practical adaptive single-phase reclosing algorithm has to consider all these conditions and perform proper operations under any system configurations or arcing conditions.

Few papers also propose a hybrid reclosing scheme suitable for UHV transmission lines in which first the faulted phase is tripped; then, the remaining two phases are tripped with a brief delay. After three phase opening, the remaining charged energy in line capacitances and inductances will feed the arc till it is consumed and arc is quenched. In this case, if the fault is transient and arc is extinguished, a sinusoidal signal with a non-zero DC offset in faulted phase voltage appears that can be simply detected as a sign of arc extinction [9][10]. Whereas, if the fault is permanent, the faulted phase voltage becomes zeros and a permanent fault can be simply detected.

The proposed algorithm in this paper uses the pattern of the faulted phase voltage in the complex plane, which is compared with the other two healthy phase voltages to distinguish between transient and permanent faults and also to detect when the arc is extinguished. Theoretical analysis is provided

to support the technique.

A typical system including transmission line, shunt reactors, CVT is simulated in EMTP. The fault arc is also properly modeled. MATLAB is used to implement and verify the algorithm. The performance of the proposed algorithm is validated by using EMTP simulation of various cases characterized by permanent and transient faults, transposed and untransposed lines, with or without four-legged reactors, using different neutral reactors, different arc parameters and different fault locations. The performance of the proposed algorithm is also verified by using data from a real transmission line.

In this paper, the theoretical analysis is presented in Section II. The system modeling is described in Section III. The observations from simulations and the analysis are given in Section IV. In Section V, the proposed adaptive reclosing algorithm is explained. The verification of the proposed algorithm is discussed in Section VI.

## II. ANALYTIC ANALYSIS

In this section, an analytic approach using steady state equivalent model with valid simplifications is employed to investigate the faulted phase voltage signal pattern after transmission line trip in case of permanent and transient faults. The resistance and conductance of the equipment are ignored as they are negligible. The source impedances at both ends of the transmission line are ignored compared to the line coupling impedance between phases. This analysis is performed for transposed and untransposed lines with or without four-legged reactor. The transmission line with neutrally grounded shunt reactor is excluded as the arc extinction time is typically long for this case and single phase reclosing is not recommended and effective [1].

### *A. Transposed Line*

#### *1) Without shunt reactor*

For a transmission line, after single phase isolation, the secondary arc current comprises of both capacitive and inductive coupling components. Figure 1 (a) shows the capacitive coupling circuit for a transposed line without shunt reactor. The rearrange and simplified circuit is shown in Figure 1 (b). In this figure, $E_x$ (x is h, k or s) is the average of phase x voltages at line ends (sending and receiving ends). This simplification is valid and helps to simplify the analytical analysis and does not impact the proposed algorithm [4].

The inductive component depends mainly on the load currents in the healthy phases, mutual inductive couplings between healthy phases and equivalent admittance of the faulted phase [5]. The inductive component can be modeled as an impedance added to a voltage source equivalent to $(E_h+E_k)/2$ (see Figure 1 (b)); nevertheless, it is negligible and consistent assuming that the healthy line load currents do not change considerably after line isolation. Since the proposed algorithm is based on the movement trend of faulted phase voltage rather than the absolute voltage magnitude and angle, it is not adversely affected by the presence of the inductive component. Hereafter, the inductive component is ignored for all the following cases.

The equivalent circuit in Figure 1 (a) is rearranged and simplified in Figure 1 (b) to obtain the faulted phase voltage. As shown in this figure, immediately after isolation of the faulted phase, the phase voltage $V_s$ drops as the line becomes isolated from the source. In this case, the faulted phase voltage can be estimated by (1).

$$V_s = \frac{R_{arc} \,||\, \left(\frac{1}{j\omega C_0}\right)}{R_{arc} \,||\, \left(\frac{1}{j\omega C_0}\right) + \frac{1}{j\omega\frac{2}{3}(C_1-C_0)}} \left(\frac{E_h+E_k}{2}\right) \quad (1)$$

Where,
$V_s$: Voltage of faulted phase at line end
$R_{arc}$: Arc resistance
$C_0$: Zero sequence capacitance of transmission line
$C_1$: Positive sequence capacitance of transmission line
$E_h$: Source voltage of healthy phase (average of both ends)
$E_k$: Source voltage of healthy phase (average of both ends)
$E_s$: Source voltage of faulted phase (average of both ends)
ω: angular velocity
j: complex operand
||: impedance parallel operand

Immediately after the trip of the faulted phase from both line ends, the arc resistance is still small compared to the line shunt capacitive impedance. Hence, (1) can be converted to (2) to estimate the faulted phase voltage ($V_s$) immediately after line faulted phase isolation. According to (2), the magnitude of $V_s$ ($|V_s|$) increases with the increase in arc resistance. In addition, the faulted phase voltage leads ($E_h+E_k$) by 90°. Since the phase angle of ($E_h+E_k$) is about -180° (180°), as shown in Figure 2, the angle of faulted phase voltage is about -90°.

$$V_s = \frac{R_{arc}}{\frac{1}{j\omega\frac{2}{3}(C_1-C_0)}} \left(\frac{E_h+E_k}{2}\right) \quad (2)$$
$$R_{arc} \ll \frac{1}{j\omega C_0} \text{ and } R_{arc} \ll \frac{1}{j\omega\frac{2}{3}(C_1-C_0)}$$

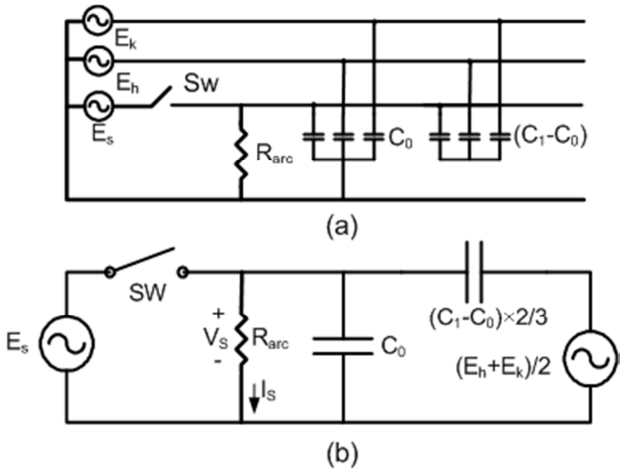


Figure 1. (a) Equivalent circuit, (b) rearranged circuit, transposed line without shunt reactor

If the fault is a permanent fault, $V_s$ would consistently lead ($E_h$+$E_k$) by 90° and $|V_s|$ stays small. However, if the fault is transient, the arc resistance would increase and the $R_{arc}$ can be treated as infinity when the arc is extinguished. Under such condition, (1) is converted to (3). According to (3), $V_s$ becomes in phase with ($E_h$+$E_k$), as shown in Figure 2.

$$V_s = \frac{2(C_1\text{-}C_0)}{2C_1+C_0}\left(\frac{E_h+E_k}{2}\right) \qquad R_{arc} \gg \frac{1}{j\omega C_0} \tag{3}$$

If transient fault is not close to the line ends, the resulting arc resistance would be higher before and right after the single pole tripping. This will result in lower voltage drop in comparison to the case of close-in fault. However, the voltage drop before the tripping is significantly lower because the line impedance is also in the fault path. Furthermore, as per (3), the angle of faulted phase voltage leads ($E_h$+$E_k$) by less than 90° after tripping due to higher arc resistance.

As defined earlier, $E_h$ and $E_k$ are the averages of phase x voltages at line ends. For a typical line protection, the voltage at remote end is not available. Therefore, the average voltage cannot be obtained. However, replacing the average voltage with the local line voltage does not adversely impact the proposed algorithm because the movement pattern between the faulted phase voltage and the healthy phase voltage will be used instead of looking at each individual voltage value. Hence, the error in phase shift or magnitude of the healthy phase voltage has little effect to the algorithm.

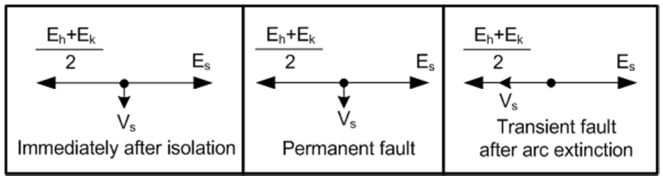


Figure 2. Phasor diagram of faulted phase voltage for a transposed line without shunt reactor

*2) With four-legged shunt reactor*

As mentioned earlier, it is a common practice to use four-legged reactors for shunt compensated lines to limit the secondary arc current for faster and successful single-phase reclosing scheme. By appropriate selection of the neutral reactor, arc current can be limited and extinguished faster [3][4]. This method is effective for transposed lines; whereas, use of switching devices and schemes for shunt reactors can be applied for untransposed lines at very high voltage levels [4]. In this paper, the analysis is not provided for four-legged reactor with switching schemes. However, the same analytical approach can be applied to those applications.

Figure 3 shows the equivalent circuit of a transposed transmission line with four-legged shunt reactor. As shown in Figure 3 (b), an inductive branch in parallel with the capacitive branch is added as compared with Figure 2(b). In order to cancel out the capacitive coupling component, inductive and capacitive branches must resonate. The neutral reactor is selected to meet this condition. Since the compensation is not ideal in practice and line cannot be treated as lumped impedance, the parallel branch is equivalent to either a large inductor or a small capacitor.

In this case, the faulted phase voltage can be estimated as below.

$$V_s = \frac{R_{arc} \,||\, \left(\frac{1}{j\omega C_0}\right) ||\left(j\omega(L_1+3L_n)\right)}{R_{arc} \,||\, \left(\frac{1}{j\omega C_0}\right) ||\left(j\omega(L_1+3L_n)\right)+Z}\left(\frac{E_h+E_k}{2}\right) \tag{4}$$

Where,

Z is the equivalent impedance of the parallel branch.

$V_s$ can be estimated by (5) at the moment after single pole tripping. As per (5), $|V_s|$ increases with the increase in arc resistance. In addition, $V_s$ lags or leads ($E_h$+$E_k$) by 90° based on the characteristic of impedance Z (inductive or capacitive respectively). Since the phase angle of ($E_h$+$E_k$) is about -180°, the angle of $V_s$ becomes about 90° in case of inductive Z or -90 degree in case of capacitive Z.

$$V_s = \frac{R_{arc}}{Z}\left(\frac{E_h+E_k}{2}\right) \qquad R_{arc} \ll \frac{1}{j\omega C_0} \text{ and } R_{arc} \ll j\omega(L_1+3L_n) \tag{5}$$

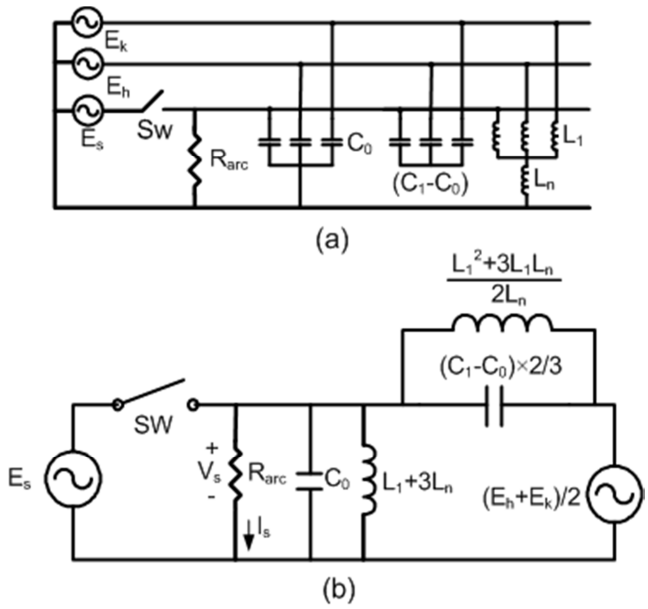


Figure 3. (a) Equivalent circuit of a transposed transmission line with four-legged shunt reactor. (b) Simplified circuit

If the fault is a permanent fault, $V_s$ would consistently lag or lead ($E_h$+$E_k$) by 90° and its magnitude stays small. However, if the fault is transient, the arc resistance would increase and when the fault arc is extinguished, $V_s$ can be estimated by (6). Normally transmission lines are shunt compensated at a level below 70%. Therefore, it is valid to assume that the equivalent impedance of the four legged shunt reactor and line zero sequence capacitance is capacitive and equal to $1/(j\omega C_{eq})$. In this case, the $V_s$ is either in phase or out of phase with ($E_h$+$E_k$).

$$V_s = \frac{\left(\frac{1}{j\omega C_{eq}}\right)}{Z}\left(\frac{E_h + E_k}{2}\right)$$
$$\frac{1}{j\omega C_{eq}} = \frac{1}{j\omega C_0} \,||\, j\omega(L_1 + 3L_n) \qquad (6)$$
$$R_{arc} \gg \frac{1}{j\omega C_0},\ R_{arc} \gg j\omega(L_1 + 3L_n) \text{ and } \frac{1}{j\omega C_{eq}} \ll Z$$

In a nutshell as demonstrated in Figure 4, if the fault is permanent, the faulted phase voltage magnitude and angle do not change with time after line isolation. Whereas, for the transient fault, the faulted phase voltage magnitude increases as the arc resistance increases till the arc is extinguished. Moreover, the angle of faulted phase voltage at the moment when the arc is extinguished lags 90° the angle of faulted phase voltage immediately after line isolation.

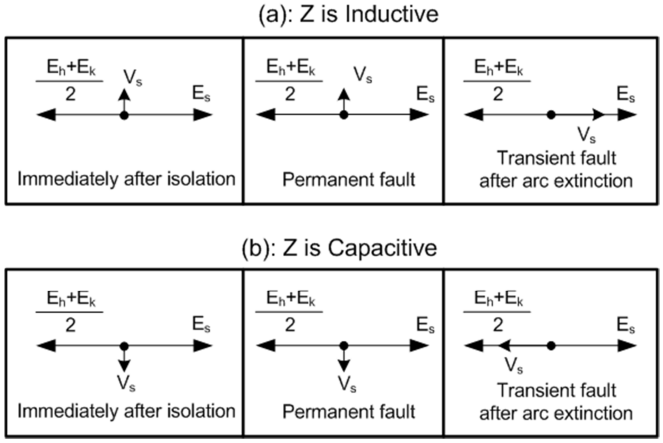


Figure 4. Phasor diagram of faulted phase voltage, transposed line with four-legged shunt reactor

### *B. Untransposed Line*

#### *1) Without shunt reactor*

Figure 5 shows the equivalent circuit of an untransposed line without shunt reactor. As shown in this figure, immediately after isolation of the faulted phase, the voltage drops since the voltage source is isolated and arc resistance is small. In general, the faulted phase voltage can be estimated as below.

$$V_s = \frac{R_{arc} \,||\, \left(\frac{1}{j\omega C_{sn}}\right)}{R_{arc} \,||\, \left(\frac{1}{j\omega C_{sn}}\right) + \frac{1}{j\omega(C_{sh} + C_{sk})}}\left(\frac{C_{sh}E_h + C_{sk}E_k}{C_{sh} + C_{sk}}\right) \qquad (7)$$

The faulted phase voltage at the moment after line isolation is obtained from the following equation:

$$V_s = \frac{R_{arc}}{\frac{1}{j\omega(C_{sh} + C_{sk})}}\left(\frac{C_{sh}E_h + C_{sk}E_k}{C_{sh} + C_{sk}}\right)$$
$$R_{arc} \ll \frac{1}{j\omega C_{sn}} \text{ and } R_{arc} \ll \frac{1}{j\omega(C_{sh} + C_{sk})} \qquad (8)$$

In case of a transient fault, when the arc is extinguished, the faulted phase voltage can be estimated as (9).

$$V_s = \frac{C_{sh}E_h + C_{sk}E_k}{C_{sh} + C_{sk} + C_{sn}}$$
$$R_{arc} \gg \frac{1}{j\omega C_{sn}} \qquad (9)$$

Comparing (7) and (1), this case is similar to the case of a transposed line without shunt reactor except that there is a phase shift because of non-transposition. As shown in Figure 6, the similar pattern can be obtained for permanent faults and transient faults.

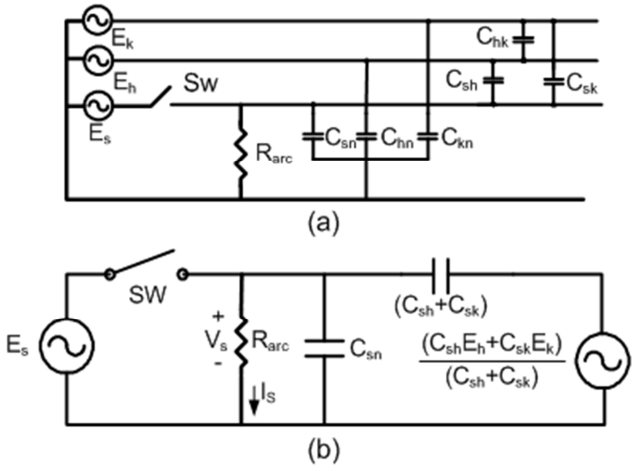


Figure 5. (a) Equivalent circuit of an untransposed transmission line without shunt reactor. (b) Simplified circuit

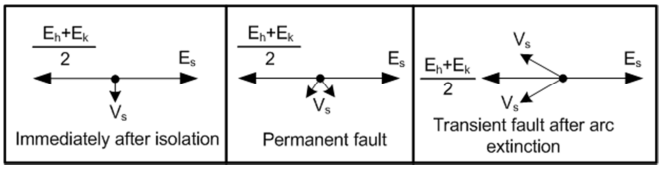


Figure 6. Phasor diagram of faulted phase voltage, an untransposed line without shunt reactor

#### *2) With four-legged shunt reactor*

Figure 7 shows the equivalent circuit (a), the rearranged circuit (b) and the simplified circuit (7) of an untransposed transmission line with four-legged shunt reactor. According to Figure 7 (c), the faulted phase voltage can be estimated as below

$$V_s = \frac{R_{arc} \,||\, \frac{1}{j\omega C_{sn}} \,||\, \left(j\omega(L_1 + 3L_n)\right)}{R_{arc} \,||\, \frac{1}{j\omega C_{sn}} \,||\, \left(j\omega(L_1 + 3L_n)\right) + Z_{eq}} E_{eq} \qquad (10)$$

Where,

$Z_{eq}$ is the equivalent impedance of the grayed circuit

$E_{eq}$ is the equivalent source of the grayed circuit

The faulted phase voltage immediately at the moment after line isolation is obtained from the following equation.

$$V_s = \frac{R_{arc}}{Z_{eq}} E_{eq}$$
$$R_{arc} \ll \frac{1}{j\omega C_{sn}},\ R_{arc} \ll j\omega(L_1+3L_n) \text{ and } R_{arc} \ll Z_{eq} \quad (11)$$

In this case, when the fault is extinguished, the faulted phase voltage can be estimated as below.

$$V_s = \frac{\left(\frac{1}{j\omega C_{eq}}\right)}{Z_{eq}} E_{eq}$$
$$\frac{1}{j\omega C_{eq}} = \frac{1}{j\omega C_0} \,||\, j\omega(L_1+3L_n) \quad (12)$$
$$R_{arc} \gg \frac{1}{j\omega C_0},\ R_{arc} \gg j\omega(L_1+3L_n) \text{ and } \frac{1}{j\omega C_{eq}} \ll Z_{eq}$$

Comparing (12) and (4), this case is also similar to that of a transposed line with four-legged shunt reactor except that there is a phase shift because of non-transposition. The same pattern as mentioned earlier applies.

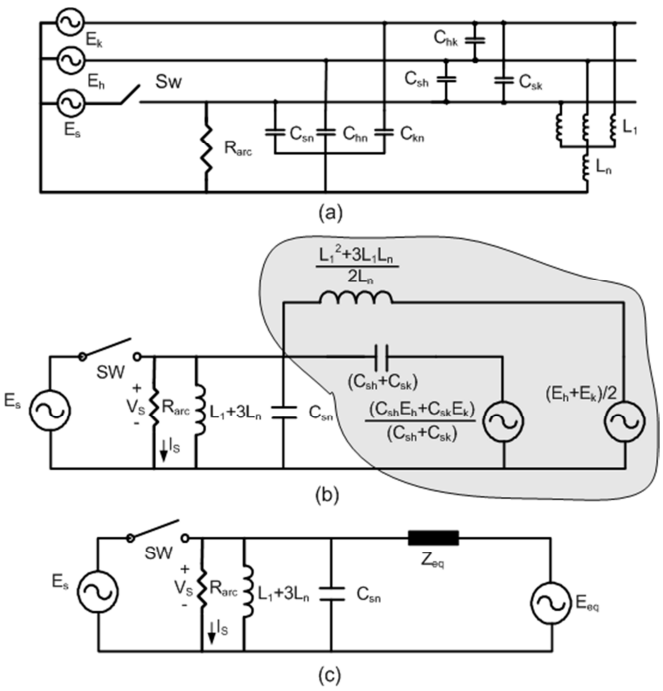


Figure 7. (a) Equivalent circuit of an untransposed transmission line with four-legged shunt reactor, (b) Rearranged circuit, (c) Simplified circuit

The approach can also be applied to the case of an untransposed line with four-legged reactor with switching schemes as proposed in [4][5]. In that case, the equivalent impedance matrix of four-legged shunt reactor is not symmetric. Nonetheless, similar equivalent circuit as Figure 7 can be obtained. Therefore, the same pattern of faulted phase voltage would apply.

In order to support the theoretical analysis, an extensive modeling and simulation study is performed. Next section describes the system modeling briefly and simulation-based analysis is presented in Section IV.

## III. System and Arc Modeling

### A. System Modeling

In this study, a typical 500 kV system with a horizontal tower configuration is simulated in EMTP. Considering the frequency range of study for the system under investigation, equivalent networks at two sides of the transmission line are modeled appropriately. The SIRs for the left and right sources are set to 0.12 and 0.175. The higher SIR results in higher short circuit current and higher ionization of the related arc thus higher arc extinction time. Wave impedances for each source are set to 200 Ω for each end. Figure 8 shows the single line diagram of the network under study.

Frequency dependent model (JMarti) is used for exact modeling of 324.3 km transmission line [11]. The line is split into three parts {30%, 40% and 30% of line length} to be able to simulate fault at {0%, 30%, 70% and 100% of line length}. Conductor positions and line configuration has been changed during the study to simulate transposed and untransposed {a-b-c, a-c-b, b-a-c} lines. In the horizontal tower configuration, a-b-c configuration means that the left conductor is a, the middle one is b and the right one is c. A three phase 158.7 MVAR reactor at each end are used to verify the performance of the proposed technique for the cases with shunt reactor. Each 158.7 MVAR reactor has been modeled by a resistance of R=5 Ω in series with a reactance of X= 1575.3 Ω. Neutral reactor is modeled by a single-phase reactance. The resistance of neutral reactor is ignored due to its negligible effect.

In order to minimize the secondary arc current, the equivalent balanced neutral reactor impedance is calculated as below [12].

$$B_1 = \omega C_1 = 0.0017 \text{ S}$$
$$B_0 = \omega C_0 = 0.0011 \text{ S}$$
$$F = \frac{1}{X_r B_1} = \frac{1}{787.65 \times 0.0017} = 0.741 \quad (13)$$
$$X_n = \frac{B_1 - B_0}{3F \times B_1 \times (B_0 - (1-F) \times B_1)} = 259.92\Omega$$

Where,

$B_1$: Positive sequence line susceptance (Siemens)
$B_0$: Zero sequence line susceptance (Siemens)
F: Shunt compensation degree
$X_r$: Equivalent reactance of line shunt reactors
$X_n$: Equivalent reactance of neutral reactors

Considering two identical four-legged shunt reactors at both ends of the simulated transmission line, the neutral reactor at each end is set to 519.8 Ω = 2×259.92 Ω. Sometimes the optimized neutral reactor may be unavailable such that neutral reactor with higher or lower impedance are actually used. In this study, as shown in Table 1, three neutral reactors were used to cover possible cases in practice. Typical resistances are selected for the selected reactors.

Since the proposed adaptive reclosing method is based on the faulted phase voltage, an appropriate CVT model is used to include any impact of CVT transient on the proposed algorithm [14].

The output of each phase of three phase CVT model is

passed through an antialiasing filter with cutoff frequency of 1920 Hz and recorded with sampling rate of 3840 Hz. The recorded data is later used in MATLAB to verify the performance of the adaptive reclosing technique.

TABLE 1. PARAMETERS OF MODELED NEUTRAL REACTORS

| Neutral Reactor | X | R |
|---|---|---|
| Balanced | 519.8 | 1.7 |
| High | 700 | 2.33 |
| Low | 300 | 1 |

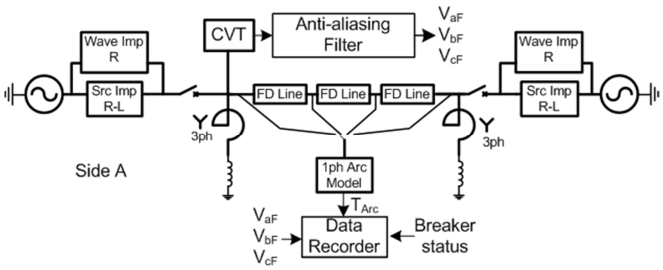


Figure 8. Single line diagram of the system under study

### B. Arc Modeling for Computer Simulation

Reproduce of the real arc behavior by computer simulation is very hard due to the extremely random characteristic of the arc. Extensive research has been performed to accurately model the arc behavior. Several input parameters required for proper arc modeling could be obtained only by measurement. Parameters extracted from measurements can be used to facilitate an arc model that reproduces the main characteristic of that specific arc measurement. Such a model might give less reliable results for other arcing conditions on the same line, or completely inaccurate results for experiments carried out on other lines with different length, voltage level and conductor arrangement [14].

However, simulation of the process that leads to the secondary arc extinction can be a valuable tool for sensitivity studies to identify the main influencing factors and to find the invariants, which are necessary to compile generalized diagrams for the estimation and detecting of the arc extinction time [15][16].

In this study, EMTP is used to model a secondary arc. As shown in Figure 9, arc resistance has been modeled as a controlled resistor between phase and ground conductors. More details about the arc modeling method are presented in [15][16][12]. The fidelity of the selected arc modeling method was validated by comparing the modeled arc with other simulations and the real arc waveforms [17][18].

Since the purpose of this paper is to analyze the faulted phase voltage pattern, an appropriate arc model with three sets of typical data that leads to three different arc models (Arc1, Arc2, Arc3) is used. Typical values for the arc parameters were taken from [17]. In addition, according to Table II, three parameters $u_0$, $l_0$ and $\tau_0$ were varied around their typical values to generate three different arcs [12].

TABLE II. ARC1, ARC2 AND ARC3 PARAMETERS

| | $u_0$ (v/cm) | $l_0$ (m) | $\tau_0$ (msec) |
|---|---|---|---|
| Arc1 | 12 | 3.5 | 0.714 |
| Arc2 | 8 | 3.15 | 0.555 |
| Arc3 | 11 | 3.5 | 0.833 |

Where,
$u_0$ is the arc characteristic voltage.
$\tau_0$ is the initial time constant.
$l_0$ is the initial arc length.

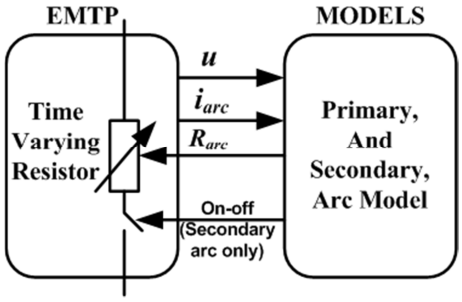


Figure 9. The method of arc modeling in EMTP, u: arc secondary voltage

## IV. SIMULATION-BASED ANALYSIS

### A. Permanent Fault

Figure 10 shows δ and $|V_s|$ for various permanent faults. δ is defined in (14). In all simulated cases, a single phase A to ground fault occurs at 0.2 second and the line is isolated from the side A at time 0.27 second and from the other side at time 0.28 second. As shown in these figures, δ varies slightly after line isolation and remains constant after that. Because of the system transients after line isolation, phasor estimation and additional filtering, it takes almost 2-4 cycles till δ becomes consistent. $|V_s|$ also drops after line isolation. Similar to δ, it takes almost 2-4 cycles for $|V_s|$ to become consistent.

$$\delta = \angle (E_h + E_k) - \angle E_s \text{ (in degree)} \quad E_h = E_b,\ E_k = E_c \text{ and } E_s = E_a \tag{14}$$

### B. Transient Faults

#### 1) Without shunt reactor

Figure 11 shows δ, $|V_s|$, and the arc current ($i_{arc}$) for the modeled transposed line without shunt reactor. In this case, arc occurs close to the Side A. As shown, δ drops immediately after line isolation at 0.28 second and then slowly increases at 0.38 second from angle -109.4° to about -11.8° and remains constant after 0.6 second. As shown in Figure 11 (c), arc is extinguished at time 0.57 and due to filtering of data and phasor estimation, the arc extinction is only recognizable by δ and $|V_s|$ not sooner than the time point of 0.6 second. This is almost the same in all the studied cases. Similarly, $|V_s|$ drops immediately after the line isolation at 0.28 second and then slowly increases at 0.38 second and remains constant after 0.6 second.

According to the simulation results, the angle of faulted phase voltage taken after arc extinction lags that taken after line isolation by 90° for transient faults. It also means that the

δ after arc extinction is 90° more than the δ after line isolation. In addition, the angle and magnitude of faulted phase voltage becomes almost constant after arc extinction. As demonstrated in Figure 11, the same pattern is found in all the simulated case. The 10° to 12° shift of δ in different simulation cases is mainly due to the replacement of the average of ($E_h$+$E_k$) with the local voltage measurement at Side A and several above-mentioned simplifications in theoretical analysis.

Figure 12 shows δ, $|V_s|$ and $i_{arc}$ for the simulated untransposed line (a-b-c) without shunt reactor. Compared with the transposed line results, the angle after line isolation and the angle after arc extinction are shifted, as compared with the case of a transposed line. However, the δ after arc extinction is still 90° greater than the δ after the line isolation. The magnitude of faulted phase voltage ($|V_s|$) also follows the same pattern as transposed lines.

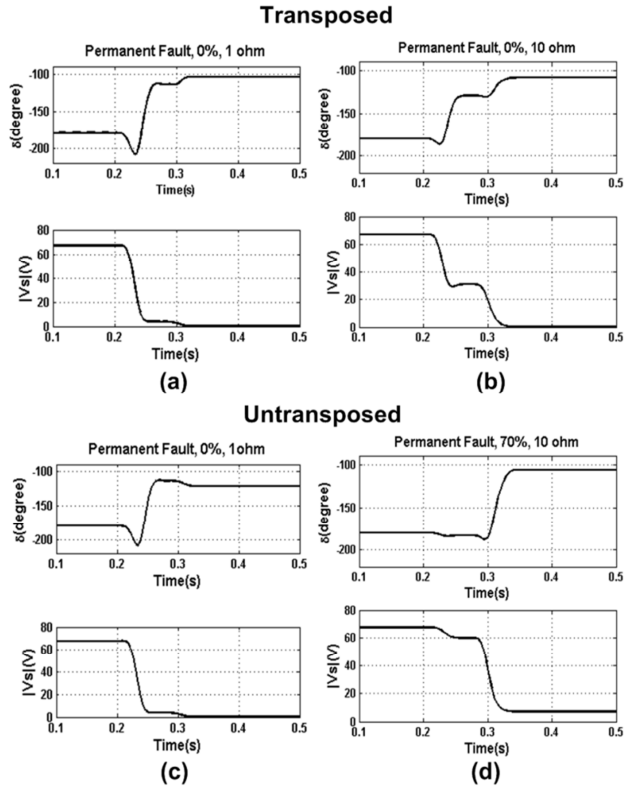


Figure 10. Faulted phase voltage pattern for various conditions in case of a permanent fault

Figure 13 is out of the same simulation configuration as used for Figure 11, except that the fault occurs at 70% of the line length. Since the fault is not a close-in fault, the arc model presents a higher resistance before and after the line isolation. In this case, δ increases immediately after line isolation without any transient drop and becomes constant after time 0.59 sec. In this case, δ after arc extinction is 66° more than δ after the line isolation. In this case, $|V_s|$ drops drastically after the line isolation due to the presence of line impedance in the fault path. After the line isolation, $|V_s|$ is slightly greater than that in the case of close-in fault because the arc resistance is higher.

*1) With shunt reactor*

Figure 14 shows δ, $|V_s|$ and $i_{arc}$ from a transposed line with four-legged shunt reactor and a close-in transient fault at Side A. As shown, δ drops immediately after line isolation at 0.28 second and then slowly increases at 0.38 second from angle -128° to about -27° at time 0.52 and becomes oscillatory afterwards. Similarly, $|V_s|$ drops immediately after line isolation at 0.28 second and then slowly increases after time 0.38 and becomes oscillatory after time 0.52 second. As it is shown in Figure 14 ($i_{arc}$), the arc is extinguished at time 0.45 and due to the filtering of data, the arc extinction can be detected from δ and $|V_s|$ at time 0.52 second where the δ and $|V_s|$ becomes oscillatory due to the resonance between line capacitances and four-legged shunt reactor. This is almost the same in all the studied cases with shunt reactor.

Figure 15 shows δ, $|V_s|$ and $i_{arc}$ from an untransposed line (a-b-c) with four-legged shunt reactor and a close-in transient fault at Side A. Compared with the case using transposed line, δ increased immediately after line isolation and the δ after arc extinction are shifted as compared to the case of a transposed line. However, the δ after arc extinction is still 100° greater than the δ after line isolation. $|V_s|$ follows the same pattern as that for untransposed line without four-legged shunt reactor.

Similar to the line without shunt reactor, if the fault is not a close-in fault, the arc resistance at the time of isolation is higher than that from a close-in fault. In this case, δ increases immediately after line isolation without any transient drop and becomes oscillatory when the arc extinguishes. The δ after arc extinction subtracted by the δ after line isolation is less than 90°. $|V_s|$ also drops drastically after line isolation and increases slowly till the arc is extinguished and $|V_s|$ becomes oscillatory.

### *C. Observations*

Based on the theoretical approach and simulation results described in Sections II and IV, the following facts were observed.

Fact 1. In case of a permanent fault, the faulted phase voltage magnitude and angle remains almost constant after line isolation after the switching transients are damped.

Fact 2. In case of a transient fault, the voltage magnitude drops immediately after the line isolation and then it slowly increases until the arc is extinguished.

Fact 3. In case of a transient fault, after the line isolation, the angle δ either drops immediately and then increases slowly, or increases from the beginning until the arc is extinguished.

Fact 4. In case of a transient fault, when the arc is extinguished, the magnitude of faulted phase voltage ($|V_s|$) either becomes constant after a small drop or becomes oscillatory with a constant DC component.

In case of a transient fault, when the arc is extinguished, the angle δ becomes constant or oscillatory with a constant DC component.

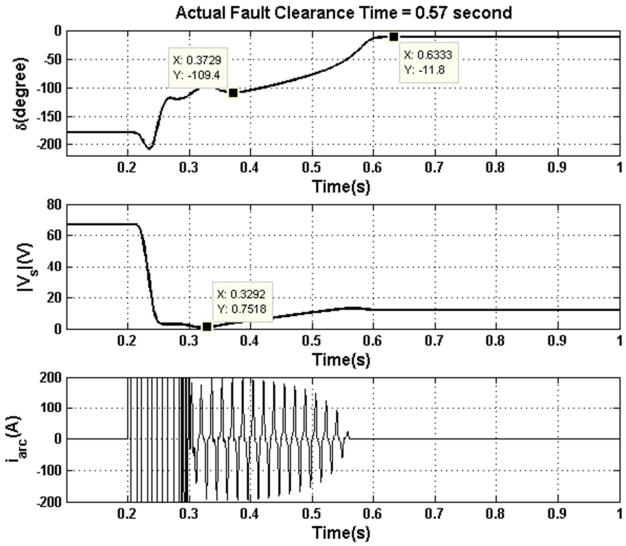


Figure 11. Faulted phase voltage and current pattern in case of a transposed line without shunt reactor and a close-in transient fault

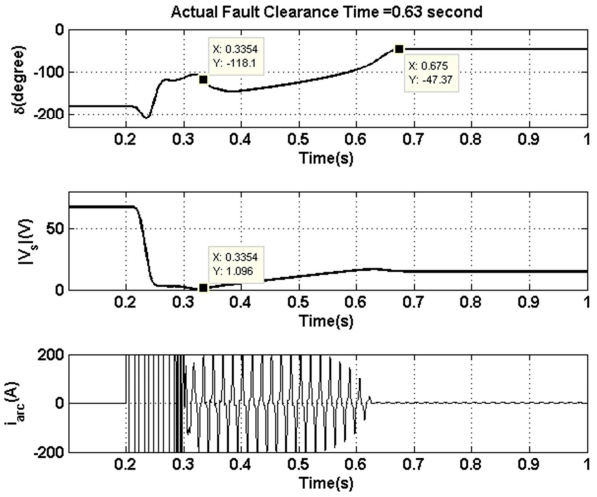


Figure 12. Faulted phase voltage and current pattern in case of an untransposed line without shunt reactor and a close-in transient fault

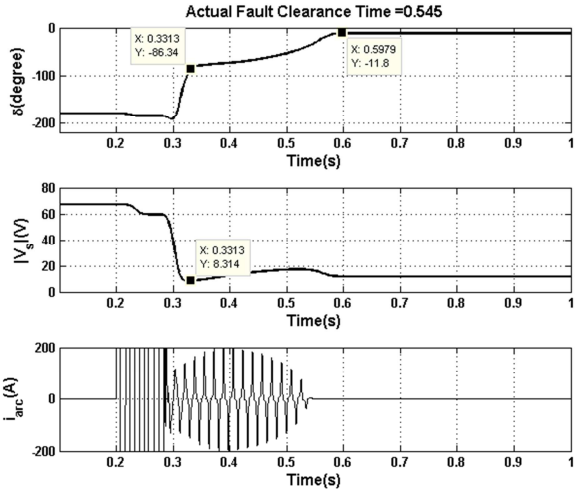


Figure 13. Faulted phase voltage and current pattern in case of a transposed line without shunt reactor and a transient fault at 70% of line length

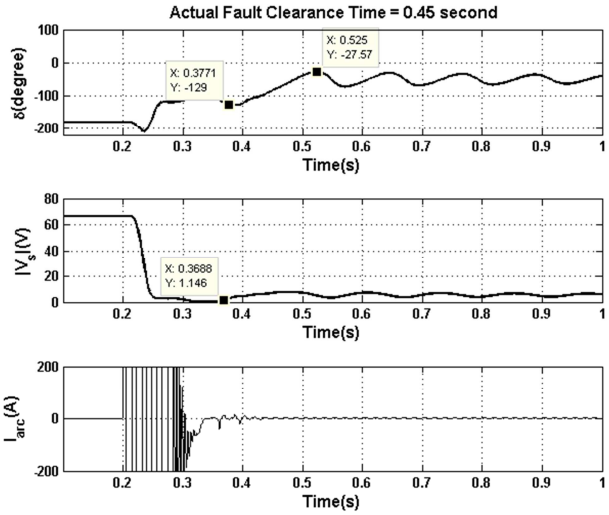


Figure 14. Faulted phase voltage and current pattern in case of a transposed line with four-legged shunt reactor and a close-in transient fault

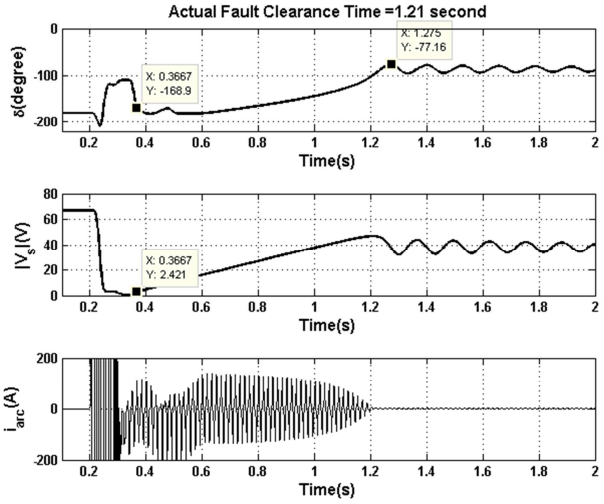


Figure 15. Faulted phase voltage and current pattern in case of an untransposed line with four-legged shunt reactor and a close-in transient fault

## V. Adaptive Reclosing Algorithm

Based on the above-mentioned facts, a new algorithm is proposed to detect a permanent fault and the time of arc extinction in case of a transient fault. Figure 16. shows the block diagram of the proposed technique. The adaptive reclosing function can be initiated either by high speed protection or the breaker open status. The breaker open status can be detected either through auxiliary contact or through CT secondary current [19]. The breaker interruption should be detected in less than two cycles in order to detect the fast extinguishing arcs. If the fault is a single-phase to ground fault, the faulted phase voltage is selected by phase selector and the adaptive reclosing algorithm can be initiated. As shown in Figure 16, it is assumed that the CVT transient filter in the line relays will be used for voltage phasor estimation.

Angle δ is calculated from (14) and compensated by ±360° to ensure that it does not encounter a shift from -180° to 180° and vice versa.

The magnitude of the faulted phase voltage ($|V_s|$) is monitored to determine the reference time ($t_{ref}$). $t_{ref}$ is the time that $|V_s|$ starts increasing after the drop that occurs after line isolation. $t_{ref}$ can be determined easily by calculation of the minimum $|V_s|$ after the initiation. If $|V_s|$ keeps to be greater than its minimum value for a cycle, the time point after that cycle and the corresponding $\delta$ are assigned to $t_{ref}$ and $\delta_{ref}$. If the reference time could not be found within 5 cycles after algorithm initiation, the time point after the 5 cycles and the corresponding $\delta$ are assigned to $t_{ref}$ and $\delta_{ref}$. The latter case normally happens only for permanent faults because the voltage magnitude does not increase after line isolation.

After algorithm initiation, $\delta$ and $|V_s|$ is low-pass filtered to attenuate all the unwanted transients above 15 Hz. Then, the long-window derivation of the filtered signals is obtained by fitting a line to the last 6 cycles of the data using least squares method [20]. The slope of the fitted line is used as a long-window derivation. This method provides a smooth and reliable estimate for derivations of $\delta$ and $|V_s|$.

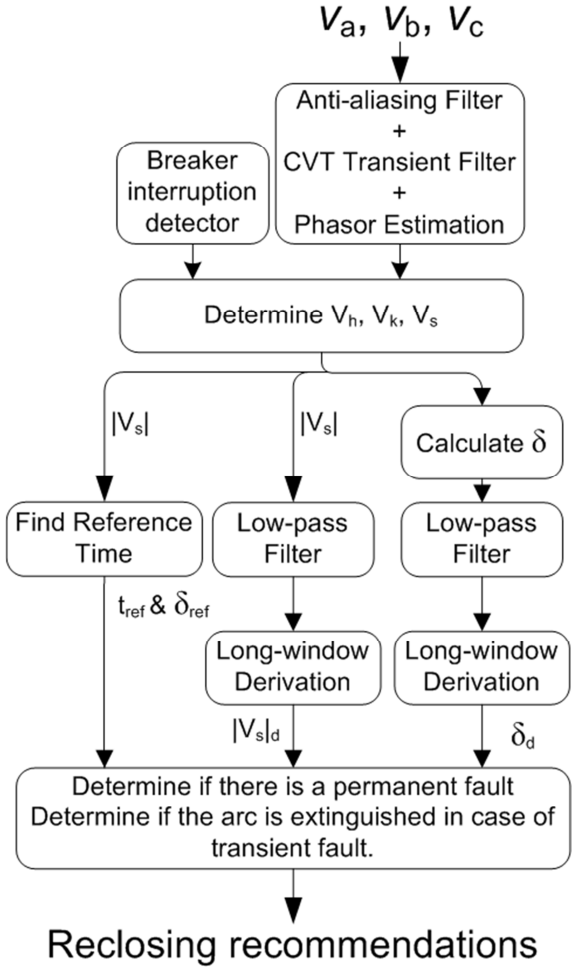


Figure 16. Block diagram of the proposed technique for adaptive reclosing

Fact 1 can be used to detect any permanent fault. This can be done by checking $\delta$, $\delta_d$ and $|V_s|_d$. If $|V_s|$ and $\delta$ remain almost constant, $\delta_d$ and $|V_s|_d$ become very small (close to zero) and ($\delta$ - $\delta_{ref}$) will be small as well (e.g. less than 10°).

Fact 2 to Fact 5 can be used to detect the transient fault and the time that arc is extinguished. As per Facts 2 and 4, $|V_s|$ slowly increases after $t_{ref}$ till the arc is extinguished. This means that, after $t_{ref}$, $|V_s|_d$ is positive till the arc is extinguished where $|V_s|_d$ either becomes negative and then zero or becomes oscillatory with a zero DC component. As per Facts 3 and 5, $\delta$ slowly increases after $t_{ref}$ till the arc is extinguished. This means that, after $t_{ref}$, $\delta_d$ is positive till the arc is extinguished where $\delta_d$ becomes zero or oscillatory with a zero DC component. Simply by checking the above-mentioned criteria, the permanent fault and transient fault with arc extinction time can be detected. Few counters and timers are also used to increase the reliability of the algorithm by checking the output of the algorithm for several time steps.

## VI. Results

In order to verify the performance of the proposed algorithm, 320 cases have been simulated in EMTP. These cases vary in line transposition, shunt reactor {no reactor, with four-legged reactor, neutral reactor with different reactance}, fault locations, and fault types.

According to the simulation results, the type of the fault is detected correctly in all 320 cases. Table 3 to Table 6 shows the average processing times required by the proposed algorithm to detect the permanent faults or the arc extinction in case of transient faults. The processing time is averaged for three different arcs as introduced in Table II.

From Table 3 to Table 6, the average processing times required by the proposed algorithm to detect the permanent faults is within 220 to 280 milliseconds. The processing time to detect the arc extinction is longer for a line without shunt reactor because $\delta_d$ becomes almost zero without reaching negative values after arc extinction. This is similar to the case of a transient fault on an untransposed line where the arc extinction process is very slow resulting in a small positive value for $\delta_d$ while the arc is still not extinguished. Distinction between these two cases requires a longer processing time. In case of a line with shunt reactor, $\delta_d$ becomes oscillatory after arc extinction and it can be quickly detected. According to the results of simulations, the average processing time in case of the line with shunt reactor is within 70 to 160 milliseconds.

In order to verify the performance of the proposed algorithm, a real transient fault recorded by a protection relay at Rockport 765kV station in American Electric Power is examined. The case is a transient fault on a 765 kV untransposed line. The line is equipped with a four-legged reactor without switching scheme at one end and a four-legged reactor with switching scheme at the other end [5]. The fault occurs at time 0.1 second; the line is isolated at time 0.145s and reclosed at 0.63 second by using the event record time reference. From the waveforms, the fault is actually extinguished at time 0.3 second. The proposed technique is applied analytically and could detect the fault type as transient and the arc extinction at time 0.41 second which is 110 milliseconds after the actual arc extinction time. Using the proposed adaptive reclosing technique, the line could have been reclosed 13 cycles faster.

TABLE 3. AVERAGE PROCESSING TIME IN CASE OF A LINE WITHOUT SHUNT REACTOR

| Average Processing Time (s) | | Without Shunt Reactor | | | |
|---|---|---|---|---|---|
| | | Fault Location (% of Line) | | | |
| | | 0 | 30 | 70 | 100 |
| Transposed Line | Transient | 0.22 | 0.22 | 0.22 | 0.22 |
| | Permanent | 0.28 | 0.22 | 0.22 | 0.22 |
| Untransposed Line (a-b-c) | Transient | 0.22 | 0.22 | 0.22 | 0.22 |
| | Permanent | 0.28 | 0.23 | 0.23 | 0.22 |
| Untransposed Line (a-c-b) | Transient | 0.22 | 0.22 | 0.22 | 0.22 |
| | Permanent | 0.28 | 0.22 | 0.22 | 0.22 |
| Untransposed Line (b-a-c) | Transient | 0.22 | 0.22 | 0.22 | 0.22 |
| | Permanent | 0.28 | 0.22 | 0.23 | 0.22 |

TABLE 4. AVERAGE PROCESSING TIME IN CASE OF A LINE WITH A BALANCED FOUR-LEGGED SHUNT REACTOR AT EACH END

| Average Processing Time (s) | | With 4-legged Shunt Reactor (Balanced) | | | |
|---|---|---|---|---|---|
| | | Fault Location (% of Line) | | | |
| | | 0 | 30 | 70 | 100 |
| Transposed Line | Transient | 0.13 | 0.16 | 0.12 | 0.07 |
| | Permanent | 0.28 | 0.23 | 0.22 | 0.22 |
| Untransposed Line (a-b-c) | Transient | 0.12 | 0.12 | 0.12 | 0.12 |
| | Permanent | 0.28 | 0.23 | 0.23 | 0.22 |
| Untransposed Line (a-c-b) | Transient | 0.12 | 0.12 | 0.12 | 0.12 |
| | Permanent | 0.28 | 0.22 | 0.22 | 0.22 |
| Untransposed Line (b-a-c) | Transient | 0.12 | 0.12 | 0.11 | 0.11 |
| | Permanent | 0.28 | 0.22 | 0.23 | 0.22 |

TABLE 5. AVERAGE PROCESSING TIME IN CASE OF A LINE WITH A HIGH FOUR-LEGGED SHUNT REACTOR AT EACH END

| Average Processing Time (s) | | With 4-legged Shunt Reactor (High) | | | |
|---|---|---|---|---|---|
| | | Fault Location (% of Line) | | | |
| | | 0 | 30 | 70 | 100 |
| Transposed Line | Transient | 0.13 | 0.16 | 0.11 | 0.08 |
| | Permanent | 0.28 | 0.23 | 0.22 | 0.22 |
| Untransposed Line (a-b-c) | Transient | 0.12 | 0.12 | 0.12 | 0.12 |
| | Permanent | 0.28 | 0.23 | 0.23 | 0.22 |
| Untransposed Line (a-c-b) | Transient | 0.12 | 0.12 | 0.12 | 0.11 |
| | Permanent | 0.28 | 0.22 | 0.22 | 0.22 |
| Untransposed Line (b-a-c) | Transient | 0.12 | 0.12 | 0.11 | 0.11 |
| | Permanent | 0.28 | 0.22 | 0.23 | 0.22 |

TABLE 6. AVERAGE PROCESSING TIME IN CASE OF A LINE WITH A LOW FOUR-LEGGED SHUNT REACTOR AT EACH END

| Average Processing Time (s) | | With 4-legged Shunt Reactor (Low) | | | |
|---|---|---|---|---|---|
| | | Fault Location (% of Line) | | | |
| | | 0 | 30 | 70 | 100 |
| Transposed Line | Transient | 0.13 | 0.13 | 0.12 | 0.12 |
| | Permanent | 0.28 | 0.23 | 0.22 | 0.22 |
| Untransposed Line (a-b-c) | Transient | 0.13 | 0.12 | 0.13 | 0.13 |
| | Permanent | 0.28 | 0.23 | 0.23 | 0.22 |
| Untransposed Line (a-c-b) | Transient | 0.13 | 0.13 | 0.12 | 0.12 |
| | Permanent | 0.28 | 0.22 | 0.22 | 0.22 |
| Untransposed Line (b-a-c) | Transient | 0.12 | 0.12 | 0.11 | 0.11 |
| | Permanent | 0.28 | 0.22 | 0.23 | 0.22 |

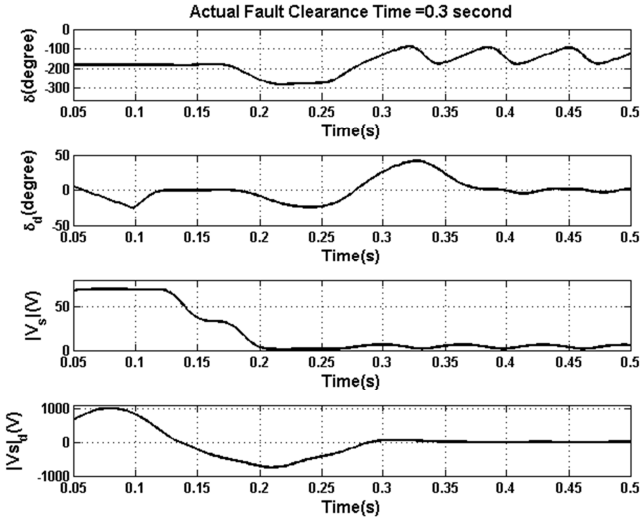


Figure 17. Secondary arc and its derivative voltage pattern in case of a recorded real single-phase to ground fault

## VII. CONCLUSIONS

A new algorithm based on the voltage pattern of line faulted phase is proposed to distinguish the permanent and transient faults in single pole tripping and reclosing application. In addition, it can detect when the arc is quenched in case of a transient fault. Theoretical approach is used to analyze the faulted phase voltage pattern in case of permanent and transient faults. Several possible cases such as transposed and untransposed lines with and without four-legged shunt reactors have been analyzed. Simulation studies including the detailed modeling of system and arc have been performed to verify the conclusion of the theoretical analysis. Five facts have been observed to distinguish between permanent and transient faults and to detect the time when the arc is extinguished. A new technique is proposed and implemented in MATLAB to simulate adaptive reclosing by interpreting the faulted phase voltage pattern based on the five facts. Altogether 320 cases have been simulated to verify the performance of the proposed technique. The performance of the proposed technique is also examined by a recorded data obtained from a real transient fault. The proposed algorithm results in correct distinguish of fault types in all the cases with about 70-280 millisecond processing time, which is significantly less than a typical reclosing time interval used in EHV and UHV transmission system.

## REFERENCES

[1] IEEE Committee Report, "Single phase tripping and auto re-closing of transmission lines," *IEEE Transactions on Power Delivery*, vol. 7, no. 1, pp. 182–192, Jan. 1992.

[2] I. M. Dudurych, T. J. Gallagher, and E. Rosolowski, "Arc effect on single-phase reclosing time of a UHV power transmission line," *IEEE Trans. on Power Delivery*, vol. 19, no. 2, pp. 854–860, April 2004.

[3] A.S. Rao and C.S. Cook, "Discussion of faults and shunt reactor parameters on parallel resonance," *IEEE Trans. on Power Apparatus and System*, vol. PAS-100, no.2, pp. 572-584, Feb. 1981.

[4] B.R. Shperling, A. Fakheri, “Single-phase switching phase parameters for untransposed EHV transmission line,” *IEEE Trans. on Power Apparatus and System*, vol. PAS-98, no.2, pp. 643-654, March 1979.

[5] A. Fakheri, B. J. Ware, B. R. Shperling, “Compensation Scheme for Single-Pole Switching on Untransposed Transmission Lines” *IEEE Transactions on Power Apparatus and Systems*, vol. PAS-97 , no. 4, pp. 1421-1429, 1978.

[6] Z. M. Radojevic´, J. Shin, “New Digital Algorithm for Adaptive Reclosing Based on the Calculation of the Faulted phase Voltage Total Harmonic Distortion Factor”, *IEEE Transactions on Power Delivery*, vol. 22, No. 1, pp. 37-41, January 2007.

[7] A. Montanari, M. C. Tavares, C. M. Portela, “Adaptive Single-Phase Auto-reclosing based on Faulted phase voltage Harmonic Signature”, International conference on Power Systems Transients, Kyoto, Japan, June 2-6, 2009.

[8] L Bin, Z. Shuo, P. Crossley, B. Zhiqian “The scheme of single-phase adaptive reclosing on EHV/UHV transmission lines”, IET 9th International Conference on Developments in Power System Protection (DPSP), pp. 116-120, 17-20 March 2008.

[9] S. Jamali A. Parham, “New approach to adaptive single pole auto-reclosing of power transmission lines”, *IET Generation, Transmission & Distribution*, vol. 4 , no. 1, pp. 115–122, 2010.

[10] S. Ahn, C. Kim, R. K. Aggarwal, A. T. Johns, “An Alternative Approach to Adaptive Single Pole Auto-Reclosing in High Voltage Transmission Systems Based on Variable Dead Time Control”, *IEEE Transactions on Power Delivery*, vol. 16, no. 4, October 2001, pp. 676-686.

[11] J.R. Marti, “Accurate modeling of frequency-dependent transmission lines in electromagnetic transient simulations,” *IEEE Trans. on Power Apparatus and Systems*, vol. PAS-101. no. 1, pp. 147-155, Jan. 1982.

[12] M.R.D. Zadeh, M. Sanaye-Pasand, A. Kadivar, “Investigation of Neutral Reactor Performance in Reducing Secondary Arc Current”, *IEEE Trans. on Power Delivery*, vol. 23, no. 4, pp. 2472-2479, 2008.

[13] H. Daqing; J. Roberts, “Capacitive voltage transformer: transient overreach concerns and solutions for distance relaying”, *Canadian Conference on Electrical and Computer Engineering*, vol. 1, 26-29 May, 1996, pp. 119–125.

[14] M.C. Tavares, and C.M. Portela, "Transmission system parameters optimization sensitivity analysis of secondary arc current and recovery voltage," *IEEE Trans. on Power Delivery*, vol. 19, no. 3, July 2004.

[15] L. Prikler, M. Kizilcay, G. Ban, P.Handl, “Improved secondary arc model based on identification of arc parameters from staged fault test records,” *14th PSCC*, Sevilla, 24-28 June 2002, Section 24.

[16] S. Goldberg, W.F. Horton , D. Tziouvaras, “A computer model of the secondary arc current in single phase operation of transmission line,” *IEEE Trans. on Power Delivery*, vol. 4 , no. 1, pp. 586-595, Jan 1989.

[17] C. Portela, N. Santiago, O. Oliveira, C. Dupont, “Modelling of arc extinction in air insulation,” *IEEE Trans. on Electrical Insulation*, vol. 27, no. 3, pp. 457 - 463, June 1992.

[18] Y. Goda, M. Iwata, K. Keda, S. Tanaka, “ Arc voltage characteristics of high current fault arcs in long gaps,” *IEEE Trans. on Power Delivery*, vol. 15, no. 2, pp. 791-795, April 2000.

[19] B. Kasztenny, V. Muthukrishnan, T.S. Sidhu, “Enhanced Numerical Breaker Failure Protection”, *IEEE Trans. on Power Delivery*, vol. 23, no. 4, pp. 1838-1845, 2008.

[20] T. Kariya and H. Kurata, *Generalized Least Squares*, Wiley, 2004.

**Mohammad R. D. Zadeh** (M’06) received B.S. and M.Sc. degrees in electrical engineering from University of Tehran in 2002 and 2005, respectively. At the same time, he worked in Moshanir Power Engineering Consultants for three years, and served as a system study engineer. He joined the University of Western Ontario, London, ON, Canada, in 2005 and received the Ph.D. in 2009. He continued as a post-doctoral fellow in the same department till January 2010. Then, he joined GE Multilin as an application engineer. Mohammad authored and co-authored more than 30 journal and conference papers at major power system journals and conferences. His areas of interest include power system protection, automation, control, and analysis.

**Ilia Voloh** received his Electrical Engineer degree from Ivanovo State Power University, Russia. He then was for many years with Moldova Power Company in various progressive roles in Protection and Control field. Since 1999 he is an application engineer with GE Multilin in Markham Ontario heavily involved in the development of UR-series relays. His areas of interest are current differential relaying, phase comparison, distance relaying and advanced communications for protective relaying. Ilia authored and co-authored more than 20 papers presented at major North America Protective Relaying conferences. He is a member of the main PSRC committee, and a senior member of the IEEE.

**Mital Kanabar** received his B.E. degree from Sardar Patel University India in 2003, and obtained his M.Tech. degree from Indian Institute of Technology (IIT) Bombay, India in 2007. He has finished his Ph.D. work at the University of Western Ontario, London, Canada in Apr. 2011, and joined GE Digital Energy, Markham from May 2011. Mital is the author of a book chapter and magazine article, as well as 3 journal and 15 conference papers. His areas of interest are synchrophasor data concentrator, wide area applications, IEC 61850 process bus, and generator protection.

**Yiyan Xue** received his B.Eng. from Zhejiang University in China and M.Sc. from the University of Guelph in Canada. With over 17 years experience in power system protection and control, he is currently employed as a senior engineer in Transmission P&C Standards group of AEP, working on protection standards, fault analysis and system simulation studies. Before joining AEP, he was an application engineer with GE Multilin providing consulting service for utilities and industrial customers. Prior to GE, he was a P&C engineer in ABB Inc. working on substation automation system design and commissioning. He is a senior member of the IEEE and a professional engineer registered in Ohio.

Previously presented at the 2010 Georgia Tech Conference